J Ginseng Res 43 (2019) 475–481

Contents lists available at ScienceDirect

Journal of Ginseng Research

journal homepage: http://www.ginsengres.org

Research Article

Ginsenoside Rg1 augments oxidative metabolism and anabolic response of skeletal muscle in mice

Hyeon-Ju Jeong [1,☆], Hyun-Kyung So [1,☆], Ayoung Jo [3,☆], Hye-Been Kim [1], Sang-Jin Lee [3], Gyu-Un Bae [3,*], Jong-Sun Kang [1,2,**]

[1] Department of Molecular Cell Biology, Samsung Medical Center, Single Cell Network Research Center, Sungkyunkwan University School of Medicine, Suwon, Republic of Korea
[2] Samsung Biomedical Research Institute, Samsung Medical Center, Seoul, Republic of Korea
[3] Research Center for Cell Fate Control, Research Institute of Pharmaceutical Science, College of Pharmacy, Sookmyung Women's University, Seoul, Republic of Korea

ARTICLE INFO

Article history:
Received 12 January 2018
Received in Revised form
12 April 2018
Accepted 25 April 2018
Available online 4 May 2018

Keywords:
Atrophy
Exercise-specific signaling
Ginsenoside
Rg1
Skeletal muscle

ABSTRACT

Background: The ginsenoside Rg1 has been shown to exert various pharmacological activities with health benefits. Previously, we have reported that Rg1 promoted myogenic differentiation and myotube growth in C2C12 myoblasts. In this study, the *in vivo* effect of Rg1 on fiber-type composition and oxidative metabolism in skeletal muscle was examined.
Methods: To examine the effect of Rg1 on skeletal muscle, 3-month-old mice were treated with Rg1 for 5 weeks. To assess muscle strength, grip strength tests were performed, and the lower hind limb muscles were harvested, followed by various detailed analysis, such as histological staining, immunoblotting, immunostaining, and real-time quantitative reverse transcription polymerase chain reaction. In addition, to verify the *in vivo* data, primary myoblasts isolated from mice were treated with Rg1, and the Rg1 effect on myotube growth was examined by immunoblotting and immunostaining analysis.
Results: Rg1 treatment increased the expression of myosin heavy chain isoforms characteristic for both oxidative and glycolytic muscle fibers; increased myofiber sizes were accompanied by enhanced muscle strength. Rg1 treatment also enhanced oxidative muscle metabolism with elevated oxidative phosphorylation proteins. Furthermore, Rg1-treated muscles exhibited increased levels of anabolic S6 kinase signaling.
Conclusion: Rg1 improves muscle functionality via enhancing muscle gene expression and oxidative muscle metabolism in mice.

1. Introduction

Skeletal muscle comprises approximately 40–50% of body weight, and the maintenance of skeletal muscle function and mass appears to be critical for metabolic homeostasis and healthy life [1]. Owing to the rapid aging of the world's population, the prevention of age-related muscle weakness and loss, termed sarcopenia, has become an important issue for public health and reducing socio-economic burden. During this process, a decline in muscle mass accompanies the loss of muscle strength, oxidative muscle metabolism, and metabolic capacity [2–4]. In addition to normal aging, various chronic diseases, including metabolic syndrome, inflammation, cardiovascular diseases, and cancers, have been linked with muscle atrophy and weakness which further exacerbate life quality and span [5]. To treat muscle atrophy, various preventive strategies, such as exercise and nutritional factors, have been investigated [6]. For the improvement of muscle mass and strength, exercise and nutritional supplements have been widely examined. Exercise has been shown to induce the activated protein kinase(AMPK)/PPARγ coactivator-1α (AMPK/PGC1α) signaling pathway, thereby enhancing mitochondrial biogenesis and oxidative muscle metabolism to improve energy efficiency and

* Corresponding author. Research Center for Cell Fate Control, Research Institute of Pharmaceutical Science, College of Pharmacy, Sookmyung Women's University, Cheongpa-ro 47-gil 100, Yongsan-Gu, Seoul 04310, Republic of Korea.
** Corresponding author. Department of Molecular Cell Biology, Samsung Medical Center, Single Cell Network Research Center, Sungkyunkwan University School of Medicine, Suwon 440-746, Republic of Korea.
E-mail addresses: gbae@sookmyung.ac.kr (G.-U. Bae), kangj01@skku.edu (J.-S. Kang).
☆ These authors contributed equally to this work.

https://doi.org/10.1016/j.jgr.2018.04.005
p1226-8453 e2093-4947/$ – see front matter

skeletal muscle strength [7–9]. The control of muscle mass involves a balancing act between protein synthesis via the mammalian target of rapamycin (mTOR)/p70 ribosomal protein S6 kinase (S6K)–mediated anabolic pathway and the protein degradation pathway via atrogin-1/muscle ring finger protein 1 E3 ubiquitin ligases [10,11]. Although physical exercise appears to be the best strategy to prevent muscle weakness, the effect of compounds or chemicals induced by exercise on skeletal muscle has been the focus. GW501516 and an analog of adenosine monophosphate (AMP) that is capable of stimulating AMP-dependent protein kinase (AMPK) activity, and GW501516 (AICAR) have been shown to enhance mitochondrial oxidative phosphorylation (OXPHOS) and muscle strength [12,13]. In a recent study, we reported that the major compound ginsenoside Rg1 promoted myoblast differentiation through the promyogenic p38 mitogen-activated protein kinase (p38MAPK)/Protein Kinase B (AKT) signaling and myotube hypertrophy through AKT/mTOR signaling [11]. Furthermore, the level of atrogin-1 and muscle ring finger protein 1 has been shown to decrease by Rg1 treatment [11]. Other studies have shown that Rg1 pretreatment prevented exhaustive exercise-induced oxidative damage in rat skeletal muscle [13–16]. In this study, we examined the effect of Rg1 on skeletal muscle fiber-type composition and muscle strength. We demonstrated that Rg1 treatment increased muscle mass and strength with the elevated expression of both oxidative and glycolytic fiber–specific myosin heavy chain types. Furthermore, Rg1 treatment upregulated the expression of OXPHOS proteins and oxidative muscle metabolism. Consistent with this muscle mass increase, Rg1-treated muscles and primary myoblasts exhibited increased levels of anabolic S6K signaling.

2. Materials and methods

2.1. Animal experiments

The animal experiments were approved by the Institutional Animal Care and Research Advisory Committee at Sungkyunkwan University School of Medicine Laboratory Animal Research Center. Eight-week-old male C57BL/6J mice purchased from Orient Bio (catalog # 000664) were maintained at ambient temperature (22°C ± 1°C) with a 12-h light–dark cycle and free access to water and food. For the Rg1 diet experiments, Rg1 (purity > 98%) was provided by Ambo Institute, Korea, and 3-month-old mice were fed a standard diet and given control or 0.4 mg/mL Rg1-containing water in volumetric bottles. The glucose levels were measured in blood from the tail by using blood glucose monitors (LifeScan Canada, Burnaby, B.C., Canada) after fasting for 16 hours with free access to water. Forelimb grip strength was assessed by using a grip strength meter (Panlab-Bioseb, Vitrolles, France). All grip strength readings (measured in g) were normalized to the animal's body weight.

2.2. Histology

For histochemical examination, freshly dissected muscles were frozen in liquid nitrogen–cooled isopentane. Transverse cryosections of skeletal muscles were obtained using a cryostat microtome (Leica, Wetzlar, Germany) and sliced into 7-μm–thick sections. The cryosections were processed for staining with Mayer's hematoxylin eosin (Sigma-Aldrich, St. Louis, MO). The nicotinamide adenine dinucleotide dehydrogenase (NADH) activity was evaluated through incubation for 30 minutes at 37°C with 0.9 mM NADH and 1.5 mM nitro blue tetrazolium (Sigma-Aldrich) in 3.5 mM phosphate buffer (pH 7.4). Succinate dehydrogenase (SDH) activity was assessed through incubation for 30 minutes with 50 mM sodium succinate and 0.3 mM nitro blue tetrazolium in 114 mM phosphate buffer containing K-EGTA (Sigma-Aldrich). For immunostaining, the muscle sections were fixed, permeabilized, and processed for incubation with primary antibodies against MHCIIA, MHCIIB, MHCIIX, (Developmental Studies Hybridoma Bank, Iowa, IA), and laminin (Abcam, Cambridge, England). After primary staining at 4°C overnight, the sections were incubated with secondary antibodies conjugated to Alexa Fluor 568 or Alexa Fluor 488 (Thermo Fisher Scientific, Waltham, MA). Images were captured by

Table 1
List of primers used for qRT-PCR

Primers	Gene accession no		Sequence (5′–3′)
L32	NM_172086.2	F	GGCCTCTGGTGAAGCCCAAGATCG
		R	CCTCTGGGTTTCCGCCAGTTTCGC
GLUT4	NM_001359114.1	F	TTCCTTCTATTTGCCGTCCTC
		R	TGGCCCTAAGTATTCAAGTTCTG
HK2 (hexokinase 2)	NM_013820.3	F	GCTGGAGGTTAAGAGAAGGATG
		R	TGGAGTGGCACACACATAAG
MTCO1	NC_005089.1	F	CTACTATTCGGAGCCTGAGC
		R	GCATGGGCAGTTACGATAAC
COX2	NC_005089.1	F	ACGAAATCAACAACCCCGTA
		R	GGCAGAACGACTCGGTTATC
SDHB	NM_001355515.1	F	ACCCCTTCTCTGTCTACCG
		R	AATGCTCGCTTCTCCTTGTAG
MB (myoglobin)	NM_001164047.1	F	CACCATGGGGCTCAGTGATG
		R	CTCAGCCCTGGAAGCCTAGC
PK (pyruvate kinase)	NM_001253883.1	F	CATGCAGCACCTGATAGC
		R	AGCTGCTGCTAAACACTTAT
PFK (phosphofructokinase)	NM_001163487.1	F	ACCAGAGGACGTTTGTGTTAG
		R	GGCGGACACTCAGGAATAAA
MHCI	NM_080728.2	F	CCATCTCTGACAACGCCTATC
		R	GGATGACCCTCTTAGTGTTGAC
MHCIIA	NM_001039545.2	F	GGCTTCAGGATTTGGTGGATAA
		R	GGATCTTGCGGAACTTGGATAG
MHCIIB	NM_010855.3	F	GATTGACGTGGAGAGGTCTAAC
		R	CCTGAGTTTCCTCGTACTTCTG
MHCIIX	NM_030679.2	F	TTCATTAGTTTCCCAGCTCTCC
		R	AGGCACTCTTGGCCTTTATC

COX2, cyclooxygenase 2; GLUT4, glucose transporter type 4; MHC, myosin heavy chain; MT-CO1, Mitochondrially Encoded Cytochrome C Oxidase I; qRT-PCR, real-time quantitative reverse transcription polymerase chain reaction; SDH, succinate dehydrogenase; SDHB, SDH complex iron sulfur subunit B.

using a Nikon ECLIPS TE-2000U and NIS-Elements F software (Nikon, Tokyo, Japan). The myofibers were traced, and their area was measured by using NIS-Elements F software (Nikon).

2.3. RNA and protein analysis

Real-time polymerase chain reaction (PCR) analysis was performed as described previously [17]. Briefly, total RNA was extracted from the powdered muscles by using easy-BLUE reagent (iNtRON Biotechnology, Seoul, South Korea) in accordance with the manufacturer's instructions and then reverse transcribed into cDNA by using PrimeScript 1st strand cDNA Synthesis Kit (Takara, Japan). Real-time PCR was performed by using SYBR Premix Ex Taq (Takara). The data were normalized to the expression of ribosomal gene L32. The primer sequences are shown in Table 1. Western blots were performed as described previously [17,18]. The total proteins were extracted from gastrocnemius (GAS) muscle by using Radioimmunoprecipitation assay (RIPA) lysis buffer (iNtRON) supplemented with a protease inhibitor tablet cocktail (Roche Diagnostics, Basel, Switzerland), separated using Sodium dodecyl sulfate polyacrylamide gel electrophoresis (SDS-PAGE), and incubated with primary and secondary antibodies. The primary antibodies used were Total OXPHOS (Thermo Fisher), phosphorylated glycogen synthase (p-GS), GS, p-S6K, S6K, p-S6, S6, phosphorylated 4E binding protein 1 (p-4EBP1), 4EBP1, heat shock protein 90 (Cell Signaling Technology, Beverly, MA), and β-tubulin (Zymed Laboratories Inc, South San Francisco, CA).

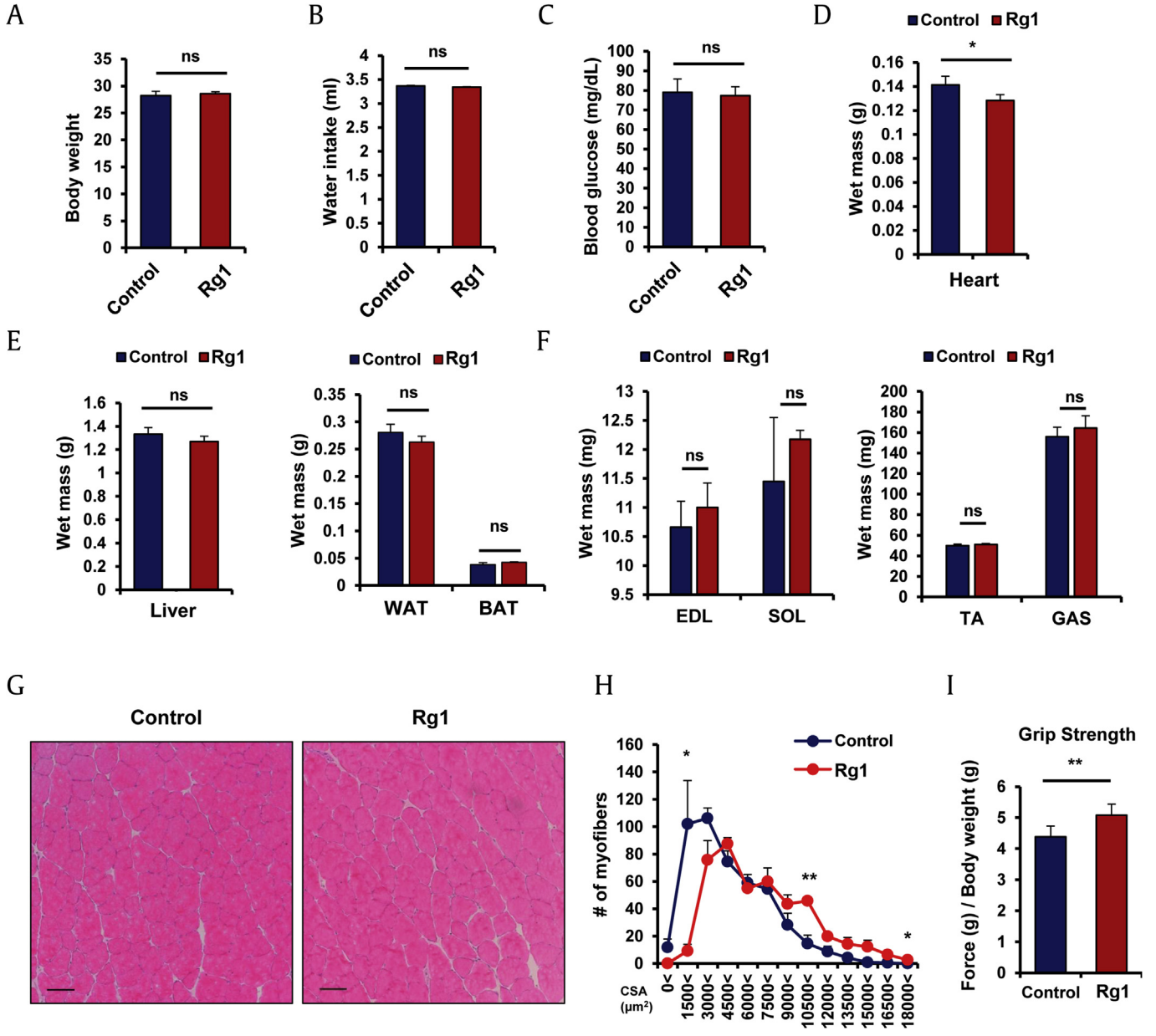

Fig. 1. Rg1 enhances muscle size and function. (A) Body weights of 3-month-old control-fed and Rg1-fed mice for 4 weeks. (B) Daily water intake from control- and Rg1-fed mice. (C) Fasting blood glucose levels over 16 h. (D) Heart weights from control- and Rg1-treated mice. (E) Liver, white adipose tissue (WAT), and brown adipose tissue (BAT) mass of control- and Rg1-treated mice. (F) Weights of four muscle types from control- and Rg1-fed mice. The data represent the mean ± SD. $^{*}p < 0.05$. ns, not significant. (n = 4–5). (G) Representative images of hematoxylin eosin–stained tibialis anterior (TA) muscle from control- and Rg1-treated mice. Scale bar = 50 μm. (H) Quantification of cross-sectional area (CSA) from the muscles of control- or Rg1-fed mice (n = 4). The data represent the mean ± SEM. $^{*}p < 0.05$, $^{**}p < 0.01$. (I) Measurement of grip strength in control- or Rg1-treated mice for 3 weeks (n = 10). The data represent the mean ± SD. $^{**}p < 0.01$. ns, not significant.
EDL, extensor digitorum longus; GAS, gastrocnemius; SD, standard deviation; SEM, standard error of mean; SOL, soleus.

2.4. Primary myoblast culture

Primary myoblasts were isolated from the hind limbs of 3–week-old mice, as described previously [19]. Briefly, the cells were cultured in F10 medium supplemented with 20% fetal bovine serum and 2.5 ng/mL basic fibroblast growth factor (Invitrogen, Carlsbad, CA). To induce differentiation, the cells were kept without the addition of fresh medium, then immunostained with myosin heavy chain (MF20, Developmental Studies Hybridoma Bank), and immunoblotted with antibodies as indicated.

2.5. Statistical analysis

The experiments were analyzed independently 3–4 times. The data are expressed as the mean ± standard deviation or ± standard error of mean, as indicated in the figure legends. The differences were considered statistically significant for p values of < 0.05 ($^{*}p < 0.05$, $^{**}p < 0.01$, $^{***}p < 0.001$).

3. Results and discussion

3.1. Rg1 enhances muscle size and function

To examine the effect of Rg1 on skeletal muscle, we first assessed the body weight, hind limb muscle size, and the mass of various organs from 3-month-old mice treated with control or Rg1 for 4 weeks. The body weight and weight of examined organs, excluding heart, did not differ between control- and Rg1-treated mice (Fig. 1A, D, E). The heart weight was slightly but significantly reduced by Rg1 treatment; this effect was consistent with that reported in previously published studies that showed the protective effect of Rg1 on cardiac hypertrophy induced by pressure overload [20,21]. In addition, the fasting blood glucose level was not significantly altered (Fig. 1C). The measurement of individual muscle mass revealed that the wet mass of all four examined muscles, the extensor digitorum longus, soleus, tibialis anterior (TA), or GAS, was slightly, but not significantly, increased (Fig. 1F).

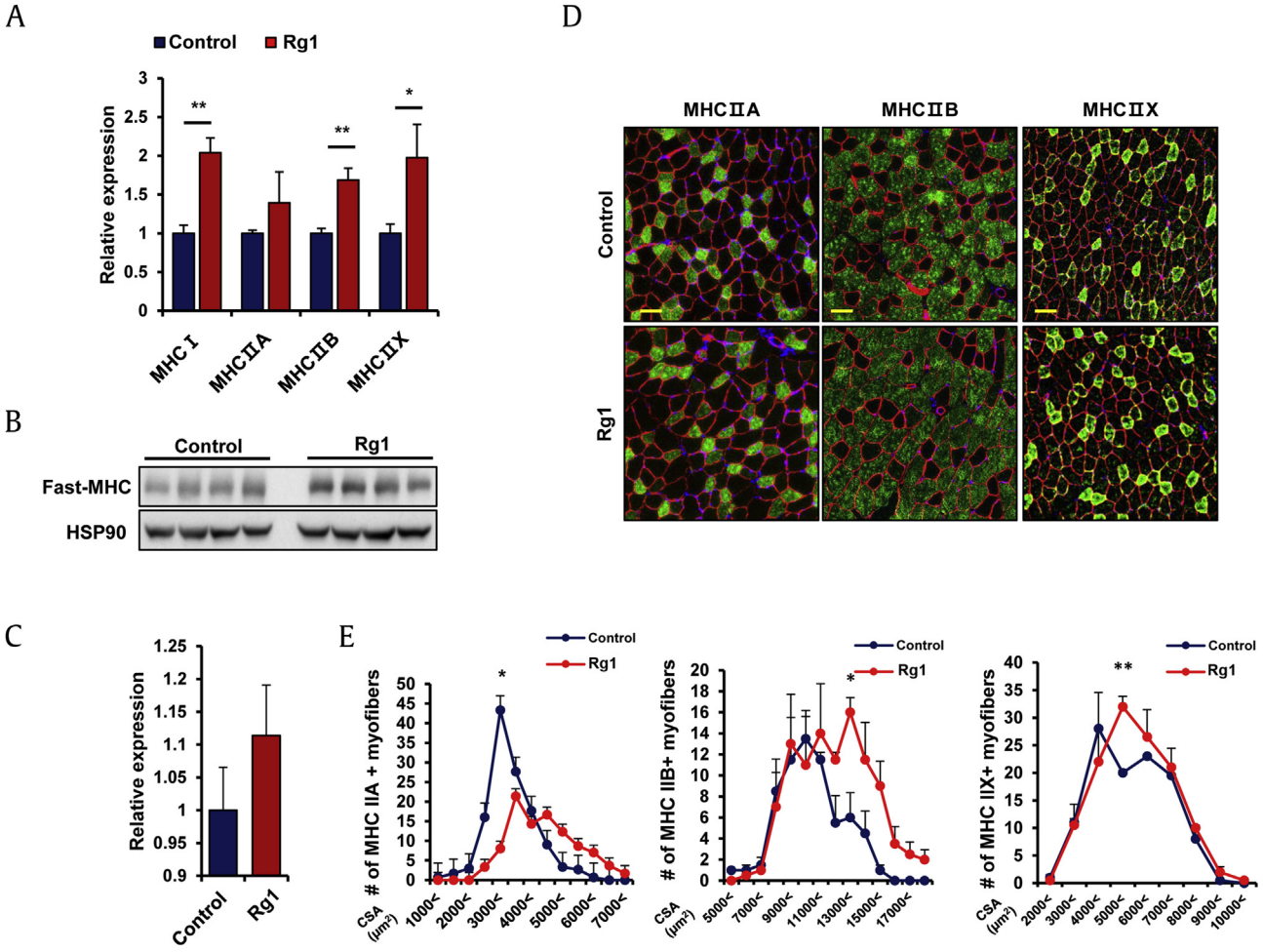

Fig. 2. Rg1 increases all muscle fiber types. (A) Real-time quantitative reverse transcription PCR (qRT-PCR) analysis of different myosin heavy chain (MHC) types from control- and Rg1-fed gastrocnemius (GAS) muscles (n = 4). The data represent the mean ± SEM. $^{*}p < 0.05$, $^{**}p < 0.01$. (B) Western blot analysis for fast MHC expression and heat shock protein 90 (HSP90) in control- and Rg1-treated GAS muscles. (C) The intensity of fast MHC was normalized to heat shock protein 90 (HSP90) as shown in panel B. The value of the control was set to 1.0. The data represent the mean ± SD. (D) Immunostaining for MHC type IIA, IIB, and IIX in control- or Rg1-treated tibialis anterior (TA) muscles. Scale bar = 50 μm. (E) Quantification of the cross-sectional area of MHC type IIA-, IIB-, and IIX-positive myofibers (n = 3–4). The data represent the mean ± SEM. $^{*}p < 0.05$, $^{**}p < 0.01$.
CSA, cross-sectional area; SD, standard deviation; SEM, standard error of mean.

However, the close histological examination of TA muscles showed larger myofibers, which likely contributed to a mild increase in muscle weight (Fig. 1G and H). Rg1-treated mice exhibited significantly elevated grip strength, as assessed by the grip test, compared with the control-treated mice (Fig. 1I). These results suggested that Rg1 treatment increased myofiber size and elevated muscle strength. These results agreed with the data as previously reported that Rg1 elicited myoblast differentiation and myotube hypertrophy in cultured C2C12 myoblasts [14].

3.2. Rg1 enhanced the expression of both glycolytic and oxidative muscle fiber markers

Skeletal muscles constitute different muscle fiber types that differ in their contractile and metabolic properties, as well as their mitochondrial content [22,23]. Based on the contractile property, myofibers are divided into slow twitch (type I) and fast twitch (type IIA, IIX, and IIB) fibers. The type I and IIA fibers use oxidative metabolism to obtain energy, whereas type IIB and IIX fibers generate Adenosine triphosphate (ATP) mainly through glycolysis [24]. Here, we examined the fiber-type composition in control- and Rg1-treated muscles. Rg1-treated GAS muscles showed significantly elevated levels of myosin heavy chain specific for type 1 fibers (MHCI), MHCIIB, and MHCIIX, which suggested that Rg1 promoted the expression of both oxidative and glycolytic myofiber genes (Fig. 2A). Consistently, the immunostaining of TA muscles for MHCIIA, IIB, and IIX revealed enlarged fibers in Rg1-treated muscles, and the measurement of individual fiber areas showed a shift to larger myofibers in Rg1-treated TA muscles (Fig. 2D and E). In addition, the immunoblot analysis of Rg1-treated GAS muscles confirmed the increased expression levels of the fast fiber–specific myosin heavy chain protein compared with those of the control muscles (Fig. 2B and C). These data suggested that Rg1 enhanced both oxidative and glycolytic muscle fibers, likely contributing to increased muscle mass and strength.

3.3. Rg1 augments oxidative muscle metabolism

Diverse stimuli, including exercise, have been shown to elevate the mitochondrial oxidative metabolic capacity of skeletal muscle, thereby enhancing muscle strength and preventing muscle atrophy [25]. To examine the mitochondrial activity, TA muscle sections were subjected to histological staining for the activities of two mitochondrial enzymes, NADH tetrazolium (NADH-TR) and SDH. The number of NADH-TR and SDH-positive fibers with stronger signal intensities was increased in Rg1 TA muscles relative to that in the control muscles (Fig. 3A and B). Then, we analyzed five proteins involved in mitochondrial OXPHOS, including NADH dehydrogenase (OXPHOS I), succinate dehydrogenase (OXPHOS II), ubiquinone cytochrome c oxidoreductase (OXPHOS III), cytochrome c, cytochrome oxidase (OXPHOS IV), and ATP synthase (OXPHOS V). In support of the histological staining results, Rg1-treated GAS muscles exhibited elevated levels of OXPHOS proteins compared with the control muscles (Fig. 3C and D). To further examine the expression of metabolic genes, GAS muscles were subjected to qRT-PCR analysis. Among the oxidative fiber–related genes, cyclooxygenase 2, SDH complex

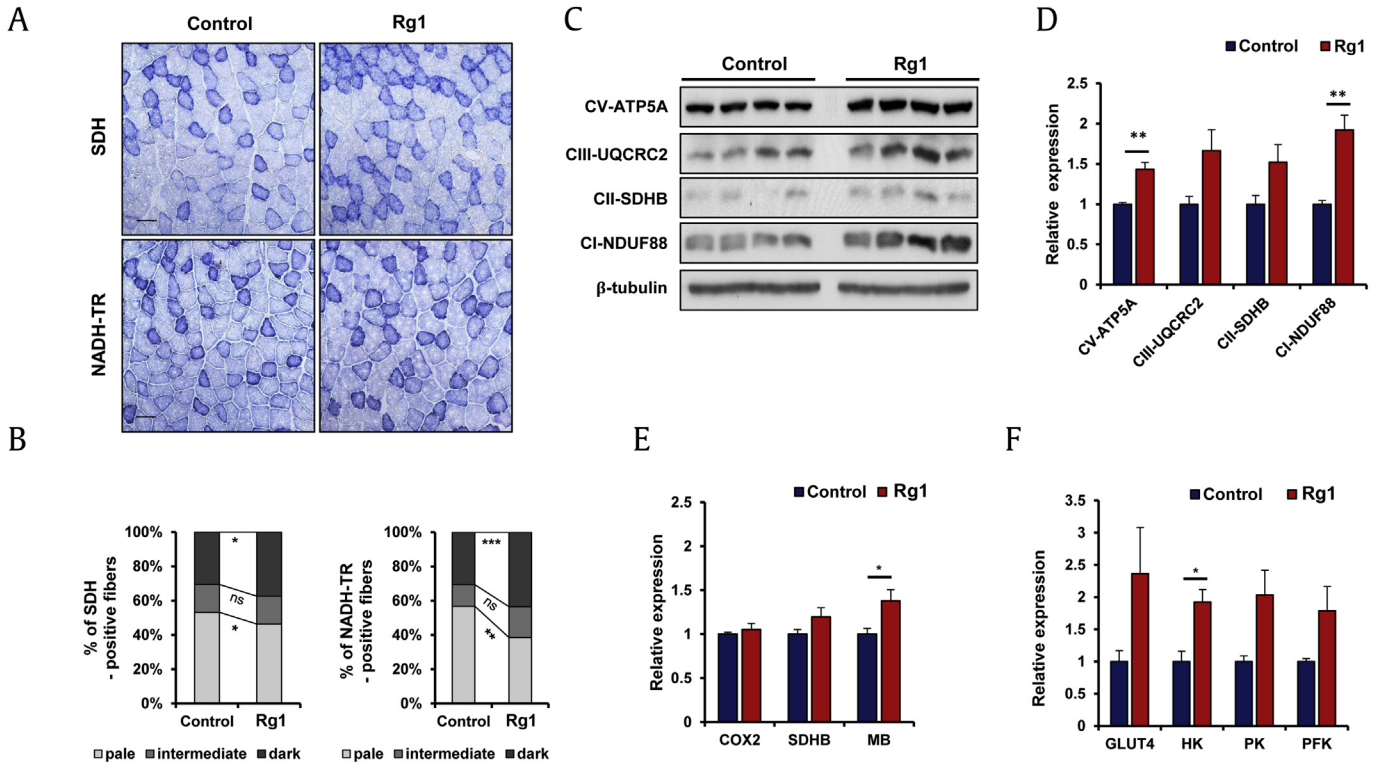

Fig. 3. Rg1 promotes the metabolic function of mitochondria in skeletal muscle. (A) Succinic dehydrogenase (SDH) and nicotinamide adenine dinucleotide dehydrogenase tetrazolium (NADH-TR) enzymatic activity in control- and Rg1-treated tibialis anterior (TA) muscles. Scale bar = 50 μm. (B) The quantification of stained myofibers by three different staining grades (n = 3). The data represent mean ± SEM. $^{*}p < 0.05$, $^{**}p < 0.01$, $^{***}p < 0.001$. (C) Immunoblotting analysis of respiratory chain components (CI–CV) from control- and Rg1-treated gastrocnemius (GAS) muscles. (D) The intensity of respiratory chain components (CI–CV) was normalized β-tubulin. The value of control-fed states were set to 1.0 (n = 4). The data represent the mean ± SD. $^{**}p < 0.01$. (E, F) Real-time quantitative reverse transcription PCR (qRT-PCR) analysis of mitochondrial and glycolytic genes in control- and Rg1-treated gastrocnemius (GAS) muscles (n = 4). The data represent thee mean ± SEM. $^{*}p < 0.05$.
COX2, cyclooxygenase 2; GLUT4, glucose transporter type 4; HK, hexokinase; MB, myoglobin; PCR, polymerase chain reaction; PFK, phosphofructokinase; PK, pyruvate kinase; SD, standard deviation; SDH, succinate dehydrogenase; SDHB, SDH complex iron sulfur subunit B; SEM, standard error of mean.

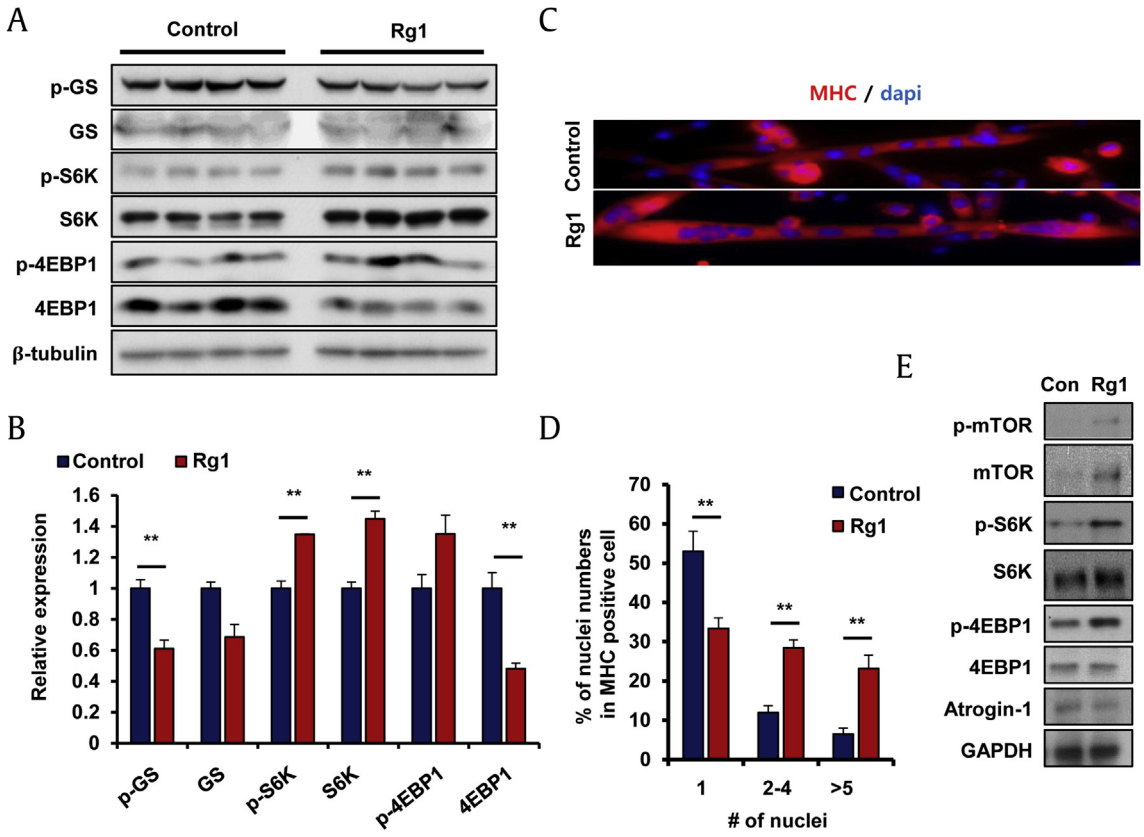

Fig. 4. Rg1 induces protein translation and inhibits atrophy in skeletal muscle. (A) Immunoblot analysis of various regulators in control- and Rg1-fed gastrocnemius (GAS) muscles. (B) The relative protein levels of phosphorylated glycogen synthase (p-GS), glycogen synthase (GS), phosphorylated S6 kinase (p-S6K), S6 kinase (S6K), phosphorylated 4E binding protein 1 (p-4EBP1), and 4E binding protein 1 (4EBP1). The intensity was normalized to β-tubulin. The value of control-fed states were set to 1.0 (n = 4). The data represent the mean ± SD. $^{**}p < 0.01$. (C) Immunostaining of myosin heavy chain (MHC) in control- and Rg1-treated primary myoblasts on differentiation day 3. (D) The quantification of myotube formation is shown in panel C. The data represent the mean ± SD. $^{**}p < 0.01$. The experiment was repeated three times, and the results were similar. (E) Immunoblotting analysis of various markers in control- and Rg1-treated primary myoblasts on differentiation day 3. DAPI, 4′,6-Diamidino-2-Phenylindole, dihydrochloride; GAPDH, Glyceraldehyde 3-phosphate dehydrogenase.
SD, standard deviation.

iron sulfur subunit B, and myoglobin, the expression of myoglobin significantly increased, whereas the expression of other genes was not greatly altered (Fig. 3E). Further analysis of the expression of genes involved in glucose metabolism, glucose transporter type 4, hexokinase, pyruvate kinase, and phosphofructokinase, revealed that Rg1 treatment elevated significantly hexokinase levels and other genes were nonsignificantly increased (Fig. 3F). Collectively, these data suggested that Rg1 treatment enhanced the expression of genes involved in mitochondrial oxidative metabolism and glycolysis.

3.4. Rg1 enhances S6K activation but inhibits 4EBP1 in skeletal muscle

The maintenance of skeletal muscle mass is regulated by the balance between protein synthesis and the degradation of muscle proteins [26]. Protein synthesis is regulated through the signaling pathways that involve the activation of S6K and the inhibition of the eukaryotic translation initiation factor 4EBP1 by phosphorylation [27,28]. To examine the regulatory pathways involved in muscle mass control, GAS muscles were subjected to immunoblot analysis for the phosphorylation of S6K and 4EBP1. As shown in Fig. 4A and B, Rg1-treated muscles had significantly enhanced levels of the phosphorylated active form of S6K. In addition, these muscles also had elevated levels of S6K proteins. In contrast, the phosphorylated inactive form of 4EBP1 was also increased, whereas the 4EBP1 protein level was significantly decreased in Rg1-treated GAS muscles compared with that in the control muscles. In addition, the phosphorylation of GS was also significantly decreased, which might reflect the active consumption of glucose. Similarly, we examined the effect of Rg1 on myotube growth in primary myoblasts. Rg1-treated primary myoblasts formed larger myotubes than the control cultures (Fig. 4C and D). In agreement with the Rg1-treated muscle data, Rg1 treatment enhanced the levels of active mTOR/S6K signaling (reflected by the level of p-mTOR and p-S6K) and inactive p-4EBP1 levels. In addition, the level of atrogin-1 implicated in protein degradation and muscle atrophy was mildly decreased in Rg1-treated myotubes compared with that in the control cultures (Fig. 4E). These data suggested that Rg1 augmented myotube growth, which might contribute to myofiber hypertrophy. In summary, the increased muscle mass and strength induced by Rg1 are likely attributable to enhanced oxidative muscle metabolism through the regulation of efficient energy consumption and increased protein synthesis via the activation of S6K and the inhibition of 4EBP1. Thus, Rg1 might be a valuable nutritional supplement for the enhancement of muscle function and the protection of muscles from atrophy.

Conflicts of interest

All authors have no conflicts of interest.

Acknowledgments

This work was supported by the National Research Foundation of Korea (NRF) grant funded by the Korean government (MSIP) (NRF-2017M3A9D8048710, NRF-2016R1A5A2945889 MRC to JSK; NRF-2017R1D1A1B03032978 to HJJ).

References

[1] Rolfe DF, Brown GC. Cellular energy utilization and molecular origin of standard metabolicrate in mammals. Physiol Rev 1997;77:731–58.
[2] Holloszy JO. Biochemical adaptations in muscle. Effects of exercise in mitochondrial oxygen uptake and respiratory enzyme activity in skeletal muscle. J Biol Chem 1967;242:2278–82.
[3] Gundersen K. Determination of muscle contractile properties: the importance of the nerve. Acta Physiol Scand 1998;162:333–41.
[4] Willis LH, Slentz CA, Bateman LA, Shields AT, Piner LW, Bales CW, Houmard JA, Kraus WE. Effects of aerobic and/or resistance training on body mass and fat mass in overweight or obese adults. J Appl Physiol 2012;113:1831–7.
[5] Wakahara T, Fukutani A, Kawakami Y, Yanai T. Nonuniform muscle hypertrophy: itsrelation to muscle activation in training session. Med Sci Sports Exerc 2013;45:2158–65.
[6] Gallagher D, Belmonte D, Deurenberg P, Wang Z, Krasnow N, Pi-Sunyer FX, Heymsfield SB. Organ-tissue mass measurement allows modeling of REE and metabolically active tissue mass. Am J Physiol 1998;275:E249–58.
[7] Czubryt MP, McAnally J, Fishman GI, Olson EN. Regulation of peroxisome proliferator-activated receptor gamma coactivator 1 alpha (PGC-1 alpha) and mitochondrial function by MEF2 and HDAC5. Proc Natl Acad Sci USA 2003;100:1711–6.
[8] Tadaishi M, Miura S, Kai Y, Kano Y, Oishi Y, Ezaki O. Skeletal muscle-specific expression of PGC-1α-b, an exercise-responsive isoform, increases exercise capacity and peak oxygen uptake. PLoS One 2011;6: e28290.
[9] Egan B, Zierath JR. Exercise metabolism and the molecular regulation of skeletal muscleadaptation. Cell Metab 2013;17:162–84.
[10] Bodine SC, Stitt TN, Gonzalez M, Kline WO, Stover GL, Bauerlein R, Zlotchenko E, Scrimgeour A, Lawrence JC, Glass DJ, et al. Akt/mTOR pathway is a crucial regulator of skeletal muscle hypertrophy and can prevent muscle atrophy in vivo. Nat Cell Biol 2001;3:1014–9.
[11] Rommel C, Bodine SC, Clarke BA, Rossman R, Nunez L, Stitt TN, Yancopoulos GD, Glass DJ. Mediation of IGF-1-induced skeletal myotube hypertrophy by PI(3)K/Akt/mTOR andPI(3)K/Akt/GSK3 pathways. Nat Cell Biol 2001;3:1009–13.
[12] Olson EJ, Pearce GL, Jones NP, Sprecher DL. Lipid effects of peroxisome proliferator-activated receptor-delta agonist GW501516 in subjects with low high-density lipoprotein cholesterol: characteristics of metabolic syndrome. Arterioscler Thromb Vasc Biol 2012;32:2289–94.
[13] Narkar VA, Downes M, Yu RT, Embler E, Wang YX, Banayo E, Mihaylova MM, Nelson MC, Zou Y, Juguilon H, et al. AMPK and PPARdelta agonists are exercise mimetics. Cell 2008;134:405–15.
[14] Go GY, Lee SJ, Jo A, Lee J, Seo DW, Kang JS, Kim SK, Kim SN, Kim YK, Bae GU. Ginsenoside Rg1 from Panax ginseng enhances myoblast differentiation and myotube growth. J Ginseng Res. 2017;41:608–14.
[15] Huang HY, Korivi M, Hsu MF, Huang CY, Hou CW, Chen CY, Kao CL, Lee RP, Lee SD, Kuo CH. Oral Rg1 supplementation strengthens antioxidant defense system against exercise-induced oxidative stress in rat skeletal muscles. J Int Soc Sports Nutr 2012;9:23. 1–7.
[16] Wang Y, Liu Q, Xu Y, Zhang Y, Lv Y, Tan Y, Jiang N, Cao G, Ma X, Wang J, et al. Ginsenoside Rg1 protects against oxidative stress-induced neuronal apoptosis through myosin IIA-actin related cytoskeletal reorganization. Int J Biol Sci 2016;12:1341–56.
[17] Jeong HJ, Lee HJ, Vuong TA, Choi KS, Choi D, Koo SH, Cho SC, Cho H, Kang JS. Prmt7 deficiency causes reduced skeletal muscle oxidative metabolism and age-related obesity. Diabetes 2016;65:1868–82.
[18] Bae GU, Lee JR, Kim BG, Han JW, Leem YE, Lee HJ, Ho SM, Hahn MJ, Kang JS. Cdo interacts with APPL1 and activates Akt in myoblast differentiation. Mol Biol Cell 2010;21:2399–411.
[19] Leem YE, Jeong HJ, Kim HJ, Koh J, Kang K, Bae GU, Cho H, Kang JS. CDO regulates surface expression of Kir2.1 K+ channel in myoblast differentiation. PLoS One 2016;11: e015870.
[20] Zhang YJ, Zhang XL, Li MH, Iqbal J, Bourantas CV, Li JJ, Su XY, Muramatsu T, Tian NL, Chen SL. The ginsenoside Rg1 prevents transverse aortic constriction-induced left ventricular hypertrophy and cardiac dysfunction by inhibiting fibrosis and enhancing angiogenesis. J Cardiovasc Pharmacol 2013;62:50–7.
[21] Tang F, Lu M, Yu L, Wang Q, Mei M, Xu C, Han R, Hu J, Wang H, Zhang Y. Inhibition of TNF-α-mediated NF-κB activation by ginsenoside Rg1 contributes the attenuation of cardiac hypertrophy induced by abdominal aorta coarctation. J Cardiovasc Pharmacol 2016;68:257–64.
[22] Buller AJ, Eccles JC, Eccles RM. Interactions between motoneurons and muscles in respect of the characteristic speeds of their responses. J Physiol 1960;150:417–39.
[23] Nunnari J, Suomalainen A. Mitochondria: in sickness and in health. Cell 2012;148:1145–59.
[24] Lee H, Kim SH, Lee JS, Yang YH, Nam JM, Kim BW, Ko YG. Mitochondrial oxidative phosphorylation complexes exist in the sarcolemma of skeletal muscle. BMB Rep 2016;49:116–21.
[25] Cannavino J, Brocca L, Sandri M, Bottinelli R, Pellegrino MA. PGC1-α overexpression prevents metabolic alterations and soleus muscle atrophy in hindlimb unloaded mice. J Physiol 2014;592:4575–89.
[26] Li JB, Wassner SJ. Protein synthesis and degradation in skeletal muscle of chronically uremic rats. Kidney Int 1986;29:1136–43.
[27] Magnuson B, Ekim B, Fingar DC. Regulation and function of ribosomal protein S6 kinase (S6K) within mTOR signalling networks. Biochem J 2012;441:1–21.
[28] Marabita M, Baraldo M, Solagna F, Ceelen JJM, Sartori R, Nolte H, Nemazanyy I, Pyronnet S, Kruger M, Pende M, et al. S6K1 is required for increasing skeletal muscle force during hypertrophy. Cell Rep 2016;17:501–13.